

Title page

Targeting effector memory T cells with a selective peptide inhibitor of Kv1.3 channels for therapy of autoimmune diseases

**Christine Beeton, Michael W. Pennington, Heike Wulff, Satendra Singh,
Daniel Nugent, George Crossley, Ilya Khaytin, Peter A. Calabresi,
Chao-Yin Chen, George A., Gutman, K. George Chandy**

*Department of Physiology and Biophysics, University of California Irvine, Irvine, California, USA (CB,
GAG, KGC)*

Bachem Bioscience Inc., King of Prussia, Pennsylvania, USA (MWP, SS, DN, GC, IK)

*Department of Medical Pharmacology and Toxicology, University of California, Davis, California, USA
(HW, CYC)*

Department of Pathology, Johns Hopkins Hospital, Baltimore, Maryland, USA (PAC)

CB and MP contributed equally to this work.

Running title page

Running Title:

Selective peptidic inhibitor of Kv1.3

Number of Text Pages:

Number of Tables: 2

Number of Figures: 5

Number of References: 63

Number of Words in the Abstract: 224

Number of Words in the Introduction: 819

Number of Words in the Discussion: 1457

Abbreviations: AAA, amino acid analysis; Aeea, amino-ethyloxy-ethyloxy-acetic acid; Amp, p-amino-L-phenylalanine; 4-AP, Boc, tert-butyloxycarbonyl; Bzl, benzyl; CNS, central nervous system; DIC, diisopropylcarbodiimide; DTH, delayed type hypersensitivity; EAE, experimental autoimmune encephalomyelitis; F6CA, fluorescein-6-carboxyl; Fmoc, 9-fluorenyl-methoxybarbonyl; $K_{Ca3.1}$, intermediate-conductance Ca^{2+} -activated K^{+} channel; K_v , voltage-gated K^{+} channel; MBP, myelin basic protein; MS, multiple sclerosis; PBMC, peripheral blood mononuclear cell; Pmp, p-phosphonomethyl-phenylalanine ShK, *Stichodactyla helianthus* toxin; T_{CM} , central memory T cell subset; T_{EM} , effector memory T cell subset; TMSBr, trimethylsilyl bromide; Tyr(PO_3H_2), p-phospho-Tyrosine.

Abstract

The voltage-gated Kv1.3 K⁺ channel is a novel target for immunomodulation of autoreactive effector memory (T_{EM}) T cells that play a major role in the pathogenesis of autoimmune diseases. We describe the characterization of the novel peptide ShK(L5) that contains L-phosphotyrosine linked via a 9 atom hydrophilic linker to the N-terminus of the ShK peptide from the sea anemone *Stichodactyla helianthus*. ShK(L5) is a highly specific Kv1.3 blocker that exhibits 100-fold selectivity for Kv1.3 ($K_d = 69$ pM) over Kv1.1 and greater than 250-fold selectivity over all other channels tested. ShK(L5) suppresses the proliferation of human and rat T_{EM} cells and inhibits IL2 production at picomolar concentrations. Naïve and central memory human T cells are initially 60-fold less sensitive than T_{EM} cells to ShK(L5) and then become resistant to the peptide during activation by up-regulating the calcium-activated K_{Ca}3.1 channel. ShK(L5) does not exhibit *in vitro* cytotoxicity on mammalian cell lines and is negative in the Ames test. It is stable in plasma and when administered once daily by subcutaneous injection (10 µg/kg) attains “steady state” blood levels of ~300 pM. This regimen does not cause cardiac toxicity assessed by continuous EKG monitoring, and does not alter clinical chemistry and hematological parameters after 2-week therapy. ShK(L5) prevents and treats experimental autoimmune encephalomyelitis and suppresses delayed type hypersensitivity in rats. ShK(L5) might have use for the therapy of autoimmune disorders.

Introduction

Autoimmune diseases afflict millions worldwide and may have a common pathogenic mechanism. Pathogenesis may involve the “awakening” of dormant disease-specific autoreactive T cells - for instance myelin-specific T cells in patients with multiple sclerosis (MS) - by molecular mimicry or other undetermined mechanisms. Once awakened, autoreactive T cells might differentiate from a naïve state into chronically activated memory T cells as a consequence of repeated autoantigen stimulation, and contribute to inflammatory damage by migrating rapidly into tissues, secreting inflammatory cytokines and exhibiting immediate effector function (Sallusto et al., 1999). Several lines of evidence support this scheme. First, a majority of myelin-specific T cells from MS patients are costimulation-independent activated effector memory (T_{EM}) T cells (Lovett-Racke et al., 1998; Markovic-Plese et al., 2001; Scholz et al., 1998; Wulff et al., 2003). Second, transfer of myelin-specific T_{EM} cells into naïve rat recipients induces experimental autoimmune encephalomyelitis (EAE), a model for MS (Beeton et al., 2001b). Third, T cells from type-1 diabetes mellitus patients specific for the disease-associated autoantigen glutamic acid decarboxylase 65 are chronically activated memory cells (Viglietta et al., 2002). Lastly, a majority of T cells in the synovium of patients with rheumatoid arthritis and in skin lesions of patients with psoriasis are T_{EM} cells, as are T cells that cause delayed type hypersensitivity (DTH) (Ezawa et al., 1997; Friedrich et al., 2000; Soler et al., 2003). Memory B cells, especially those belonging to the class-switched $CD27^+IgD^-$ subset, also likely contribute to the pathogenesis of many autoimmune diseases (Corcione et al., 2004; Iglesias et al., 2001; O'Connor et al., 2001). Therapies that target T_{EM} and class-switched memory B cells without impairing the activity of other lymphocyte subsets would therefore target the pathogenic cells in patients with autoimmune diseases but without compromising acute immune responses.

An exciting new therapeutic target for immunomodulation of T_{EM} and class-switched memory B cells is the voltage-gated Kv1.3 K^+ channel. T_{EM} cells up-regulate Kv1.3 upon activation and their antigen-driven proliferation is exquisitely sensitive to Kv1.3 blockers (Wulff et al., 2003). Naïve and T_{CM} cells in contrast are significantly less sensitive to Kv1.3 blockers to begin with and rapidly become resistant to Kv1.3 blockade by up-regulating the calcium-activated K^+ channel $K_{Ca}3.1$ (Chandy et al., 2004; Wulff et al., 2003). B cells, like T cells, change their potassium channel dependence from $K_{Ca}3.1$ to Kv1.3 as they differentiate from naïve into class-switched $CD27^+IgD^-$ memory B cells (Wulff et al., 2004). Kv1.3 blockers inhibit the proliferation of these cells without affecting naïve and $CD27^+IgD^+$ memory B cells. By targeting T_{EM} cells and class-switched memory B cells with Kv1.3 blockers, it might be possible to ameliorate autoimmune diseases without compromising the bulk of the immune response. The functionally restricted tissue distribution of Kv1.3 and the fact that *in vivo* Kv1.3 blockade ameliorates EAE, bone resorption in periodontal disease and DTH in animal models without causing obvious side effects has enhanced Kv1.3's attractiveness as a therapeutic target (Beeton et al., 2001b; Koo et al., 1997; Valverde et al., 2004). Although Kv1.3 blockers would suppress all activated T_{EM} (for example T_{EM} cells specific for vaccine antigens) and class-switched memory B cells, a Kv1.3-based therapy would be a significant improvement over current therapies that broadly and indiscriminately suppress the entire immune system. An additional advantage of Kv1.3 blockers is that they are reversible. Thus, one could titrate the therapeutic effect of Kv1.3 blockers when needed and stop therapy in the face of infection, unlike chemotherapeutic agents or targeted monoclonal antibody therapies, which take months to subside.

Despite extensive efforts selective and potent inhibitors of the Kv1.3 channel have not been developed (Chandy et al., 2004). The most potent Kv1.3 inhibitor is the peptide ShK from the Caribbean sea anemone *Stichodactyla helianthus* (Pennington et al., 1995). ShK blocks Kv1.3 ($K_d \sim 10$ pM), suppresses proliferation of T_{EM} cells at picomolar concentrations (Wulff et al., 2003) and ameliorates EAE (Beeton et al., 2001b). A potential drawback of ShK is its affinity (K_d 28 pM) for the neuronal Kv1.1 channel (Kalman et al., 1998). Although no side effects were observed with ShK in EAE trials (Beeton et al., 2001b), ingress of high concentrations of ShK into the brain could lead to unwanted neurotoxicity. Other inhibitors including correolide, trans-PAC, CP-339818, UK-78282, Psora-4, margatoxin (MgTX) and luteolin are less selective for Kv1.3 (Chandy et al., 2004). The development of a more selective ShK derivative is therefore necessary.

We have developed ShK(L5), a synthetic analog of ShK which blocked Kv1.3 with picomolar affinity and exhibited greater than 100 fold selectivity for Kv1.3 over Kv1.1 and other channels. Selectivity was achieved by attaching a negatively charged L-phosphotyrosine (L-*p*Tyr) via a hydrophilic linker to ShK-Arg¹. ShK(L5) suppressed T_{EM} cell proliferation *in vitro* at picomolar concentrations without compromising the function of naïve and T_{CM} cells. In proof-of-concept *in vivo* studies, ShK(L5) ameliorated EAE caused by the transfer of myelin-specific T_{EM} cells into naïve rat recipients and suppressed the DTH response also caused by T_{EM} cells. ShK(L5) may have use as a therapy for multiple sclerosis and other T- and B-cell mediated autoimmune diseases.

Materials and Methods

Synthesis of ShK Analogs. For the Fmoc-Pmp analogs, the ethyl protecting groups were removed by treating the Fmoc-Pmp(Ethyl)₂-OH with aqueous 6N HCl at reflux. After 16 hrs, a white solid precipitated out, which was isolated by filtration and washed with water until the washings were neutral (Hammerschmidt and Hanbauer, 2000). Partial removal of the ethyl protecting groups from Pmp-phosphonate resulted in either Pmp, Pmp-Et or Pmp(Ethyl)₂. All Fmoc-amino acid derivatives were obtained from Bachem A.G. (CH-4416 Bubendorf, Switzerland) except for Fmoc-D-TyrPO₃(Bzl)-OH (Nova Biochem, San Diego, CA), Fmoc-Pmp(Ethyl)-OH and Fmoc-D-Pmp(Ethyl)₂-OH (Chem Impex, Wood Dale, IL). Solid-phase assembly was initiated with Fmoc-Cys(Trt)-2-chlorotrityl resin to minimize potential racemization of the C-terminal Cys residue (Fujiwara et al., 1994). Automated assembly was carried out on an ABI-431A peptide synthesizer (Applied Biosystems, Foster City, CA). Fmoc-Aeea-OH was coupled to the N-terminus following the assembly of ShK. The resin was divided into 9 aliquots. Either Fmoc-Tyr(PO₃Bzl)-OH, Fmoc-D-Tyr(PO₃Bzl)-OH, Fmoc-Tyr(PO₃Me₂)-OH, Fmoc-Pmp-OH, Fmoc-D-Pmp-OH, Fmoc-Pmp(Ethyl)-OH, Fmoc-Pmp(Et)₂-OH, Fmoc-Tyr(tert-butyl)-OH, or Fmoc-Amp(Boc)-OH was coupled using DIC (diisopropylcarbodiimide) and HOBT (1-hydroxybenzotriazole) to one of the resin aliquots. The de-blocked peptide resin was cleaved and deprotected with reagent K (King et al., 1990) containing 5% triisopropylsilane for 2 h at RT. Met(O) was reduced by addition of solid NH₄I to the cleavage cocktail at t-15 min. (Nicolas et al., 1995). For the peptide containing Tyr(PO₃Me₂)-OH, a cleavage cocktail containing 1 M TMSBr in TFA (trifluoroacetic acid) containing thioanisole as a scavenger for 18 hr at 4° C was used (Tian et al., 1993). Incomplete removal of the methyl protecting groups is common when using this method and two of the species (Tyr(PO₃H₂) and Tyr(PO₃HMe)) are

easily purified by RP-HPLC. The Tyr(PO₄Me₂) containing analog was cleaved via standard Reagent K cleavage keeping both Me groups intact. In each case, the cleavage mixture was filtered and the crude peptide was precipitated into ice-cold diethyl ether. The precipitate was collected, yielding approximately 75 mg of peptide from 200 mg of resin. The crude product was dissolved in 20 ml of 50% aqueous AcOH and diluted into 0.75 l of H₂O. The pH of the solution was adjusted with NH₄OH to 8.2, and it was allowed to fold overnight with the addition of glutathione (2mM:1mM) (reduced:oxidized). All analogs were purified using RP-HPLC using a linear gradient of water versus acetonitrile buffered with trifluoroacetic acid as described previously (Pennington et al., 1995; Pennington et al., 1996a; Pennington et al., 1996b). Pure fractions were pooled and lyophilized, resulting in a trifluoroacetate salt of each peptide. Purity of the peptides was greater than 95%. Each sample was confirmed by RP-HPLC, AAA and MALDI-TOF MS and adjusted to account for peptide content prior to bioassay. ShK and margatoxin were obtained from Bachem Biosciences, (King of Prussia, PA). Luteolin was purchased from Sigma (St Louis, MO).

Ion channels. We used the IUPHAR nomenclature for the ion channels described in this paper (Gutman et al., 2003). Cells stably expressing *mKv1.1*, *rKv1.2*, *mKv1.3*, *hKv1.5* and *mKv3.1* have been described (Grissmer et al., 1994). Cell lines stably expressing other mammalian ion channels were gifts from several sources: *mKv1.7* in CHL cells and *hKCa2.3* in COS7 cells from Aurora Biosciences Corp., San Diego, CA; *hKv1.4* in LTK cells from Michael Tamkun, Univ. Colorado, Boulder; *hKv2.1* in HEK293 cells from Jim Trimmer, UC Davis; *Kv11.1* (HERG) in HEK293 cells from Craig January, Univ. Wisconsin, Madison; HEK293 cells expressing *hKCa1.1* or *rKCa2.1* or *hKCa3.1* from Khaled. Houamed, Univ. Chicago, IL; *hNav1.4* in HEK-293 cells from Frank Lehmann-Horn, Univ. Ulm, Germany and *Cav1.2* in

HEK-293 cells from Franz Hofmann, Munich, Germany. RBL-2H3 (expressing *Kir2.1*) and N1E-115 neuroblastoma cells (expressing *Nav1.2*) were obtained from ATCC. *hKv1.6* and *rKv3.2* (both in pcDNA3) were obtained from Protinac GmbH (Hamburg, Germany) and transiently-transfected into COS-7 cells with Fugene-6 (Roche) according to the manufacturers' protocol.

Lymphoid cells and cell lines. Histopaque-1077TM gradients (Sigma, St Louis, MO) were used to isolate splenocytes from Lewis rats and human peripheral blood mononuclear cells (PBMCs) from the blood of healthy volunteers. Human myelin oligodendrocyte glycoprotein- or tetanus toxoid-specific T_{EM} cells were generated as described (Wulff et al., 2003). The encephalitogenic CD4⁺ Lewis rat T cell line PAS (Beraud et al., 1993) was a gift from Evelyne Béraud (Univ. Marseille, France), and RPMI 8226 plasmacytoma cells were a gift from Shastri Gollapudi (UC Irvine). Jurkat and Burkitt cells were purchased from ATCC (Manassas, VA).

Electrophysiological analysis. Experiments were conducted in the whole-cell configuration of the patch-clamp technique. K_V currents were elicited by 200 ms depolarizing pulses from a holding potential of -80 mV to 40 mV as described (Bardien-Kruger et al., 2002; Kolski-Andreaco et al., 2004; Vennekamp et al., 2004; Wulff et al., 2000; Zhou et al., 1998). Each channel blocker was tested at multiple concentrations. The measured reduction in peak current at 40 mV for each concentration was used to generate a dose-response curve and the *K_d* and Hill coefficient determined with Microcal Origin software as described (Bardien-Kruger et al., 2002; Kolski-Andreaco et al., 2004; Vennekamp et al., 2004; Wulff et al., 2000; Zhou et al., 1998). The *K_d* was also determined from the on- (*T_{ON}*) and off- (*T_{OFF}*) rates for channel-block. After stabilization of peak Kv1.3 current amplitude 70 pM ShK(L5) was perfused onto the cell, and peak current values plotted as a function of time were fitted to a single exponential function to

determine T_{ON} . After reaching equilibrium-block perfusion was switched back to blocker-free bath solution. Peak currents were plotted as described above to determine T_{OFF} . K_{ON} , K_{OFF} and K_d were calculated assuming a simple bimolecular reaction between ShK(L5) and Kv1.3: $K_{ON} = 1 - T_{ON} \times K_{OFF} / (T_{ON} \times \text{ShK(L5) concentration})$; $K_{OFF} = 1 / T_{OFF}$; $K_d = K_{OFF} / K_{ON}$ (Peter et al., 2001). For Kv11.1 channels, current block was measured both at 20 mV and -50 mV (tail current). For K_{Ca} channels, $K_{ir2.1}$, and swelling-activated chloride currents we measured the change in slope conductance by the ShK analogs and for Na^+ and Ca^{2+} currents the reduction of minimum current.

Staining for flow cytometry and fluorescence microscopy. The T cell phenotypes of human PBMCs, rat splenocytes and PAS T cells were determined by flow cytometry. PBMCs were triple-stained with anti-CD3 antibody conjugated to Cy-chrome (BD Pharmingen, San Diego, CA), anti-CD45RA antibody conjugated to phycoerythrin (BD Pharmingen, San Diego, CA) and anti-CCR7 antibody conjugated to FITC (R&D Systems, Minneapolis, MN). Rat splenocytes and PAS T cells were double-stained with anti-CD3 antibody conjugated to Cy-chrome and anti-CD45RC antibody conjugated to FITC (BD Pharmingen, San Diego, CA). The stained cells were analyzed with a FACScan (BD Biosciences, San Jose, CA).

Two approaches were used to evaluate Kv1.3 protein expression in PAS T cells. First, PAS cells were stained with ShK-F6CA (10 nM, Bachem Bioscience Inc.), a fluorophore-tagged ShK analog, and analyzed by flow cytometry as described (Beeton et al., 2003). For competition experiments, PAS cells were pre-incubated with excess unlabeled ShK(L5) (100 nM) before addition of 10 nM ShK-F6CA. Second, PAS cells were permeabilized and stained with anti-Kv1.3 antibody (Koch et al., 1997) (gift from Hans-Gunther Knaus, Innsbruck, Austria) followed by a secondary antibody conjugated to Alexa-488 (Molecular Probes, Eugene, OR). Stained cells

were visualized with a Zeiss LSM-510 META confocal microscope, fluorescence intensities were measured for individual cells ($n = 10-15$) and statistical analysis carried out using the Mann-Whitney U-test.

Functional studies. Proliferation of human and rat T cells was determined with [^3H]-thymidine incorporation assays as described (Beeton et al., 2001a; Beeton et al., 2001b; Wulff et al., 2003). For measurements of IL2 production, PAS T cells were activated with MBP in the presence or the absence of ShK or ShK(L5) for 8 hours and the culture supernatants collected as described (Beeton et al., 2001a). IL2 was detected in supernatants using the rat IL2 Quantikine kit (R&D Systems, Minneapolis, MN) according to manufacturer's instructions. Effect of exogenous IL2 (20 u/ml; Sigma, St Louis, MO) on proliferation of PAS T cells was determined as described (Beeton et al., 2001a).

Circulating half-life determination and plasma stability. Known amounts of ShK(L5) were added to Lewis rat serum and the blocking activity on Kv1.3 channels tested by patch-clamp to establish a standard dose-response curve. Serum samples from Lewis rats obtained at various times after single subcutaneous or intravenous injections of ShK(L5) were tested for Kv1.3 blocking activity by patch-clamp and the levels of ShK(L5) determined from the standard curve as described (Beeton et al., 2001b). In other experiments, Lewis rats received single daily injections of 10 $\mu\text{g/kg}$ ShK(L5) and serum levels of ShK(L5) were determined 24 hours after each injection on days 1-5. To determine plasma stability of ShK(L5), rat plasma spiked with a known amount of ShK(L5) was incubated at 37°C for varying durations and then tested for Kv1.3 blocking activity; the amount of residual ShK(L5) in these samples was determined from the standard curve.

Cytotoxicity assays and Ames test. Human PBMCs, PAS, Jurkat, RPMI 8226, and Burkitt cells were grown for 48 hours in the presence or the absence of 100 nM ShK(L5). Cells were then stained with the Live/dead[®] viability/cytotoxicity kit (Molecular Probes) according to the manufacturer's instructions and the percent of live and dead cells was determined using a fluorescence microplate reader (CytoFluor, Applied Biosystems, Foster City, CA). Triton X-100 (0.1%) was used as a positive control for cell death. For the Ames test, the mutagenic activity of ShK(L5) was determined on the *Salmonella typhimurium* tester strain TA97a by Nelson Laboratories (Salt Lake City, UT).

EKG studies to evaluate cardiac toxicity. Electrocardiographic studies with implanted EKG transmitters (Data Sciences International, Arden Hills, MN) were used for heart rate variability analysis in animals that received ShK(L5) or vehicle. Experimental protocols were reviewed and approved by the Institutional Animal Care and Use Committee of UC Davis. Six Lewis rats (9-11 weeks old; weight = 219 ± 9 g) were anesthetized with a mixture of ketamine (80 mg/kg) and xylazine (7.5 mg/kg) administered by intramuscular injection. EKG transmitters were placed in the peritoneal cavity of each rat and two EKG leads were tunneled subcutaneously to the right shoulder and to the xyphoid space caudal to the ribcage. An analgesic, carprofen (5 mg/kg, subcutaneous) was administered at the end of surgery. Two weeks after surgery we performed baseline EKG recording on the rats for 2 hours (day 1). We then injected the vehicle (PBS + 2% rat serum) subcutaneously and continued recording for another 8 hours. The animals were then returned to their rooms. On day-2 we performed baseline EKG recording for 2 hours following which ShK(L5) (10 µg/kg dissolved in vehicle) was injected subcutaneously and EKG recording continued for another 8 hours. Data recorded from 1.5 hr to 3.5 hr after the injections were used for standard heart rate variability parameters-analysis in both

time and frequency domains using Nevokard software (Bio-Impedance Technology, Inc., Chapel Hill, NC).

Sub-chronic toxicity studies. Lewis rats (9-11 weeks old; weight = 199 ± 7 g) received subcutaneous injections of ShK(L5) 10 $\mu\text{g/kg/day}$ ($n = 6$) or saline ($n = 6$) for 2 weeks. Rats were weighed daily. The Comparative Biology Laboratory at University of California, Davis performed chemical (COBAS MIRA Plus, Roche Diagnostic Systems, Branchburg, NJ) and hematological (HEMAVET[®] 850 Multispecies Hematology Analyzer, CDC Technologies, Oxford, CT) analysis on blood samples drawn at the end of 2-weeks. Single-cell suspensions prepared from thymuses and spleens removed from 6 animals given ShK(L5) and 6 given saline were stained with antibodies specific for various T and B cell markers (BD Pharmingen, San Diego, CA) and analyzed by flow cytometry.

Prevention and treatment of acute adoptive EAE and prevention of DTH in Lewis rats. Female inbred Lewis rats 9-11 weeks old were purchased from Harlan-Sprague Dawley (Indianapolis, IN) and housed under barrier conditions with irradiated rodent chow and acidified water *ad libitum*. All experiments were in accordance with NIH guidelines and approved by the University of California, Irvine, Institutional Animal Care and Use Committee. ShK(L5) was dissolved in PBS + 2% Lewis rat serum (saline) for subcutaneous injection. Acute adoptive EAE was induced as described (Beeton et al., 2001a; Beeton et al., 2001b) with $6-8 \times 10^6$ myelin basic protein (MBP)-activated PAS cells. MBP was extracted from frozen guinea pig spinal cords (Harlan Bioproducts, Indianapolis, IN) as described (Deibler et al., 1972). Rats were weighed daily and observed twice daily for clinical signs of EAE. For prevention trials, rats received 10 $\mu\text{g/kg/day}$ ShK(L5) from days 0 to 5 while control rats received saline. For treatment trials,

administration of ShK(L5) (10 µg/kg/day) or saline was begun after the onset of disease (rats had a limp tail, were hunched, and had lost 6% or more of their weight over 24 hours) and continued for 3 days.

For DTH trials, Lewis rats were immunized with an emulsion of ovalbumin in complete Freund's adjuvant (Difco, Detroit, MI). Seven days later, they received an injection of ovalbumin dissolved in saline in the pinna of one ear and saline in the other ear. Rats then received subcutaneous injections of ShK(L5) (10 µg/kg/day) or vehicle (PBS + 2% Lewis rat serum). Ear swelling was measured 24 and 48 hours later using a spring-loaded micrometer (Mitutoyo, Spokane, WA).

Results

ShK(L5), a novel ShK analog that exhibits 100-fold selectivity for Kv1.3 over Kv1.1.

ShK blocks the neuronal Kv1.1 channel and the Kv1.3 channel with roughly equivalent potency. Neurotoxicity is therefore a concern under circumstances that compromise the blood-brain barrier and allow the entry of sufficient amounts of ShK to block Kv1.1 channels. Our strategy to design a Kv1.3-specific inhibitor was guided by our finding that ShK-F6CA containing fluorescein-6-carboxylate (F6CA) attached through a 20 Å-long Aeea linker to the N-terminus of ShK exhibited 80-fold selectivity for Kv1.3 over Kv1.1 (Beeton et al., 2003). Since F6CA can exist as a restricted carboxylate or also as a cyclized lactone, it was not clear whether ShK-F6CA's Kv1.3 specificity was due to the negative charge of F6CA, the hydrophobicity created by this large bulky fluorescein nucleus, potential planar π - π electronic stacking or a combination of all of these potential contributions. To distinguish between these possibilities and with the intention of developing a non-fluorescent Kv1.3-selective inhibitor, we generated a series of 12 novel N-terminally-substituted ShK analogs to probe some of these interactions. By attaching tyrosine, phenylalanine or their derivatives (varying in charge, size and hydrophobicity) through an Aeea linker to the N-terminus of ShK, we could probe the effects of charge and hydrophobicity to gain insight into our selectivity enhancement seen with F6CA substitution.

In the example shown in Figure 1A, L-phosphotyrosine (L-*p*Tyr) a negatively charged (net charge -2) post-translationally modified aromatic amino acid, was attached via the AEEA linker to ShK-Arg¹ to generate a novel analog called ShK(L5). ShK and ShK(L5) were tested on Kv1.3 and Kv1.1 channels stably expressed in L929 cells. Figure 1B shows the effects of ShK and ShK(L5) on Kv1.3 and Kv1.1 currents elicited by 200 ms depolarizing pulses from a holding potential of -80 mV to 40 mV. Both peptides reversibly blocked Kv1.3 and Kv1.1 in a dose-

dependent manner with Hill coefficients of 1 (Figs. 1B–1D). K_d s were determined from the dose-response curves shown in Figure 1C using Microcal Origin software. ShK blocked Kv1.3 ($K_d = 10 \pm 1$ pM) and Kv1.1 ($K_d = 28 \pm 6$ pM) with roughly equivalent potency as expected (Fig. 1C). In contrast, ShK(L5) was 100-fold selective for Kv1.3 ($K_d = 69 \pm 5$ pM) over Kv1.1 ($K_d = 7.4 \pm 0.8$ nM) (Figs. 1B, 1C). The time course of Kv1.3 current block by ShK(L5) and its washout is shown in Figure 1D. The time constant (T_{ON}) of ShK(L5) wash-in was 131 ± 21 sec ($n = 7$) while the time constant (T_{OFF}) for peptide wash-out was 150 ± 28 sec ($n = 4$). The K_d (57 ± 7 pM) calculated from the K_{ON} ($15 \times 10^6 \pm 0.5 \times 10^6$ M⁻¹sec⁻¹) and K_{OFF} (0.0059 ± 0.0013 sec⁻¹) values is consistent with the K_d (69 ± 5 pM) determined with Microcal Origin software.

Other ShK analogs were tested on Kv1.3 and Kv1.1 channels (Fig. 1E). ShK(D5) containing D-phosphotyrosine (D-*p*Tyr) was 35-fold selective for Kv1.3 over Kv1.1 but was an order of magnitude less potent than ShK(L5). ShK(L6) containing L-*p*Tyr-monomethyl showed modest (11-fold) Kv1.3 specificity, while ShK analogs containing L-*p*Tyr-dimethyl or L-Tyr were not selective for Kv1.3 over Kv1.1 (Fig. 1E). Analogs that contained phenylalanine or its derivatives (varying in bulk, π electron density and charge) were modestly specific or not specific for Kv1.3 over Kv1.1 (Fig. 1E). ShK(L5)'s 100-fold specificity for Kv1.3 over Kv1.1 is greater than that of ShK-F6CA (80-fold), ShK(D5) (35-fold), ShK-Dap²² (33-fold) or any other ShK analog tested (Fig. 1C).

ShK(L5) is a highly specific Kv1.3 inhibitor. We assessed ShK(L5)'s specificity on a panel of 20 ion channels (Table 1). ShK(L5) blocked the Kv1.3 channel in T cells with a K_d (76 pM) equivalent to its K_d on the cloned channel (69 pM). It was 100-fold selective for Kv1.3 over Kv1.1, 260-fold selective over Kv1.6, 280-fold selective over Kv3.2, 680-fold selective over Kv1.2 and >1000-fold selective over all other channels tested. Importantly, it was 1600-fold

Kv1.3-selective over KCa3.1, the calcium-activated K^+ channel that regulates activation of human naïve and T_{CM} cells (Wulff et al., 2003). Native ShK was less selective than ShK(L5). ShK was 2.8-fold selective for Kv1.3 ($K_d = 10 \pm 1$ pM) over Kv1.1 ($K_d = 28 \pm 6$ pM), 20-fold selective over Kv1.6 (200 ± 20 pM), 500-fold selective over Kv3.2 ($K_d = 5,000 \pm 1,000$ pM), and >1000-fold selective-over Kv1.2 (10 ± 1 nM) and KCa3.1 ($K_d = 28 \pm 3$ nM). Margatoxin, a peptide from scorpion venom that has been touted as a specific Kv1.3 inhibitor (Koo et al., 1997; Lin et al., 1993; Middleton et al., 2003) was also not specific. It was 5-fold selective for Kv1.3 (110 ± 12 pM) over Kv1.2 ($K_d = 520 \pm 1$ pM), 9-fold selective over Kv1.1 (10 ± 1 nM) and > 1000-fold selective over Kv1.6 and Kv3.2 ($K_d > 100$ nM). Luteolin, a nutraceutical sold for autoimmune diseases (www.lutimax.com) on the basis of it being a Kv1.3 inhibitor (Lahey and Rajadhyaksha, 2004), blocked Kv1.3 weakly ($K_d = 65 \pm 5$ μ M) and exhibited no selectivity over Kv1.1 ($K_d = 77 \pm 5$ μ M), Kv1.2 ($K_d = 63 \pm 4$ μ M) or Kv1.5 ($K_d = 41 \pm 3$ μ M). ShK(L5)'s exquisite specificity for Kv1.3 together with its picomolar affinity for the channel makes it a potentially attractive immunosuppressant.

ShK(L5) preferentially and persistently suppresses human T_{EM} cell proliferation. To assess ShK(L5)'s *in vitro* immunosuppressive activity we compared its ability to suppress anti-CD3 antibody-stimulated proliferation of human T_{EM} cell lines versus human PBMCs that contain a mixture of naïve and T_{CM} cells. Flow cytometry confirmed the cell surface phenotypes of the two populations studied. The T_{EM} lines were >90% CCR7⁺CD45RA⁻ (Fig. 2A), while PBMCs contained 65 % CCR7⁺CD45RA⁺ (naïve) and 18% CCR7⁺CD45RA⁻ (T_{CM}) cells (Fig. 2B). Figure 2C shows that ShK(L5) and ShK were 60-fold more effective in suppressing the proliferation of T_{EM} cells ($IC_{50} = \sim 80$ pM) compared with PBMCs ($IC_{50} = 5$ nM, $p < 0.05$). The lower sensitivity of PBMCs might be explained by a rapid up-regulation of KCa3.1 channels in

naïve and T_{CM} cells upon stimulation as has been reported previously (Ghanshani et al., 2000; Wulff et al., 2003). In keeping with this interpretation, PBMCs activated for 48 hours to up-regulate KCa3.1 expression, then rested for 12 hours, and re-activated with anti-CD3 antibody were completely resistant to ShK(L5) block (Fig. 2D, upper arrow). PBMCs that had been suppressed by ShK(L5) during the first round of stimulation exhibited identical resistance to ShK(L5) when the cells were washed, rested and re-challenged with anti-CD3 antibody. These results corroborate an earlier report showing that naïve and T_{CM} cells escape Kv1.3 inhibitors by up-regulating KCa3.1 channels (Wulff et al., 2003). Thus, ShK(L5) preferentially and persistently suppresses the proliferation of T_{EM} cells.

ShK(L5) inhibits proliferation of and IL2 production by rat T_{EM} cells; exogenous IL2 partially over-rides suppression. As a preamble to evaluating ShK(L5)'s therapeutic effectiveness we examined its ability to suppress proliferation of a memory T cell line, PAS, that causes an MS-like disease in rats (Beraud et al., 1993). As a control, we used rat splenic T cells. To confirm the differentiation status of the two cell populations we assessed the expression of CD45RC, a marker of naïve T cells (Bunce and Bell, 1997). Rat splenic T cells were 76% CD45RC⁺ (i.e. mainly naïve cells) whereas PAS cells were CD45RC⁻ suggesting that they are memory cells (Fig. 3A). To determine whether PAS cells are in the T_{EM} - or the T_{CM} -state we examined Kv1.3 expression before and 48 hours after activation. T_{EM} but not T_{CM} cells are expected to significantly up-regulate Kv1.3 levels upon stimulation (Beeton et al., 2001b; Beeton et al., 2003). Patch-clamp experiments revealed a striking increase in Kv1.3 current amplitude after MBP-stimulation of PAS cells consistent with their being T_{EM} cells (Fig. 3B). As an independent measure of the number of Kv1.3 channels on PAS cells, we used ShK-F6CA, a fluorescently labeled ShK analog that binds specifically to Kv1.3 (Beeton et al., 2003). The

intensity of ShK-F6CA staining determined by flow cytometry reflects the number of Kv1.3 tetramers expressed on the cell surface (Beeton et al., 2003). ShK-F6CA (10nM) staining intensity increased with MBP-activation of PAS cells and an excess of unlabeled ShK(L5) (100 nM) competitively inhibited ShK-F6CA staining (Fig. 3C). As a final test, we performed confocal microscopy on quiescent and MBP-stimulated PAS cells that had been fixed and stained with a Kv1.3-specific antibody. In keeping with data in Figs. 3B and 3C, resting PAS T cells had a Kv1.3 staining intensity of 4.4 ± 0.6 and this value increased to 10.6 ± 2.3 ($p < 0.005$) after antigen-induced activation (Fig. 3D) showing augmentation in Kv1.3 protein expression following activation. Thus, MBP-activated PAS cells are CD45RC⁻ Kv1.3^{high} T_{EM} cells whereas rat splenic T cells used in our experiments are predominantly in the naïve state.

MBP-triggered proliferation of PAS cells was suppressed ~1000-fold more effectively by ShK(L5) and ShK ($IC_{50} = \sim 80$ pM) than mitogen-induced proliferation of rat splenic T cells (Fig. 3E, $IC_{50} \approx 100$ nM; $p < 0.05$). These results corroborate the findings with human T cells (Fig. 2). ShK(L5) inhibited MBP-induced IL2 production by PAS cells (Fig. 3F), and exogenous IL2 partially over-rode ShK(L5) suppression of PAS cell proliferation (Fig. 3G). Earlier studies reported similar findings with less specific Kv1.3 inhibitors on human, rat and mini-pig T cells (Beeton et al., 2001a; Chandy et al., 1984; Koo et al., 1997). In summary, ShK(L5) is a powerful and selective inhibitor of human and rat T_{EM} cells, and may therefore have therapeutic use in autoimmune diseases by preferentially targeting T_{EM} cells that contribute to the pathogenesis of these disorders (Chandy et al., 2004).

ShK(L5) plasma values following subcutaneous administration. Before embarking on *in vivo* studies in a rat EAE model, we used a patch-clamp bioassay to ascertain whether circulating levels of ShK(L5) following subcutaneous injection were sufficient to inhibit T_{EM} cells. Serum

samples from ShK(L5)-treated and control rats were tested for blocking activity on Kv1.3 channels. Control serum did not exhibit detectable blocking activity indicating an absence of endogenous channel blockers. To standardize the assay, known amounts of ShK(L5) were added to rat serum and these samples were tested on Kv1.3 channels. The spiked serum samples blocked Kv1.3 currents in a dose-dependent fashion (K_d 77 ± 9 pM) that was indistinguishable from ShK(L5)'s effect in the absence of serum (Fig. 4A). Levels of ShK(L5) in treated animals were determined by comparison with the standard curve. ShK(L5) was detectable in serum 5 minutes after a single subcutaneous injection of 200 μ g/kg (Fig. 4B). Peak levels (12 nM) were reached in 30 minutes and the level then fell to a baseline of about 300 pM OVER 420 minutes (Fig. 4B). The disappearance of ShK(L5) from the blood could be fitted by a single exponential (Fig. 4C). The circulating half-life was estimated to be ~50 min.

Since the peak serum level after 200 μ g/kg (12 nM) significantly exceeds the requirement for selective blockade of Kv1.3 channels and T_{EM} cell function, we tested lower doses. After a single injection of 10 μ g/kg the peak serum concentration of ShK(L5) reached \approx 500 pM within 30 min (data not shown), a concentration sufficient to block >90% Kv1.3 but not affect Kv1.1. Repeated daily administration of this dose (10 μ g/kg/day) resulted in steady-state levels of ~300 pM (measured 24 hours after injection, Fig. 4D), which is sufficient to cause 60-70% suppression of T_{EM} cells with little effect on naïve/T_{CM} cells. The “steady-state” level is unexpected given the estimated circulating half-life of ~50 min and indicates that ShK(L5) “accumulates” on repeated administration. To determine whether the “depot” was in the skin or elsewhere in the body, we measured blood levels of ShK(L5) 10 hours after rats received single intravenous or subcutaneous injections of 10 μ g/kg ShK(L5). The peptide disappeared with the same time course following administration by either route (Fig. 4E) indicating that the skin is not

responsible for the steady-state level of 300 pM ShK(L5) reached after a single 10µg/kg daily injection (Fig. 4D), and the depot(s) resides elsewhere.

Our success in achieving a steady-state level of 300 pM ShK(L5) following daily single injections of 10µg/kg/day suggests that the peptide may be stable *in vivo*. To examine its stability we incubated ShK(L5) in rat plasma or in PBS containing 2 % rat plasma at 37°C for varying durations and then measured Kv1.3 blocking activity. In both sets of spiked samples (plasma and PBS) we observed a 50% reduction in Kv1.3-blocking activity in about 5 hours, presumably due to peptide binding to the plastic surface of the tube, and the level then remained steady for the next 2-days (Fig. 4F). As an added test of stability we compared the Kv1.3- versus Kv1.1-blocking activities of sera from ShK(L5)-treated rats. If ShK(L5) is modified *in vivo*, either by dephosphorylation of *p*Tyr or cleavage of the Acea-*p*Tyr side-chain, it would yield ShK(L4) and ShK respectively, neither of which is selective for Kv1.3 over Kv1.1 (Fig. 1E). Serum samples from ShK(L5)-treated animals exhibited the same selectivity for Kv1.3 over Kv1.1 as ShK(L5), indicating that the peptide does not undergo the modifications stated above. Taken together, these results indicate that ShK(L5) is remarkably stable in plasma and attains pharmacologically relevant serum concentrations after single daily subcutaneous injections of 10 µg/kg.

Toxicity studies. We conducted several *in vitro* and *in vivo* tests to determine if ShK(L5) exhibits any toxicity (Table 2). Human and rat lymphoid cells incubated for 48 hours with a concentration (100 nM) of ShK(L5) >1200 times greater than the Kv1.3 half-blocking dose or the IC₅₀ for T_{EM} suppression (70-80 pM), exhibited minimal cytotoxicity. The same high concentration of ShK(L5) was negative in the Ames test on tester strain TA97A suggesting that it is not a mutagen. Both *in vitro* tests failed to detect any significant toxicity.

Drug-induced blockade of Kv11.1 (HERG) channels has contributed to major cardiac toxicity and the withdrawal of several medications from the market. ShK(L5) has no effect on Kv11.1 channels at 100 nM (>1430 -fold the K_d for Kv1.3), and our chosen therapeutic regimen (10 $\mu\text{g/kg/day}$, 300 pM steady-state circulating level) should therefore not cause cardiotoxicity. As a further test, we performed heart rate variability analysis in conscious rats administered vehicle (PBS + 2% rat serum) on day-1, followed by 10 $\mu\text{g/kg/day}$ ShK(L5) on day-2. ShK(L5) had no effect on heart rate or the standard HRV (heart rate variability) parameters in both time and frequency domains (Task force of the European Society of Cardiology and the North American Society of Pacing Electrophysiology, 1996).

Encouraged by the acute toxicity experiments, we performed a sub-chronic toxicity study in which rats were administered daily subcutaneous injections of 10 $\mu\text{g/kg}$ ShK(L5) or vehicle for 2 weeks ($n = 6$ in each group). ShK(L5)-treated animals gained weight to the same degree as rats receiving vehicle (Table 2). Hematological and blood chemistry analysis showed no difference between ShK(L5)- and vehicle-treated rats, and flow cytometric analysis revealed no differences in the proportions of thymocyte or lymphocyte subsets (Table 2). Collectively, these studies suggest that ShK(L5) is safe.

To determine the therapeutic safety index, we administered a 60-fold higher dose (600 $\mu\text{g/kg/day}$) of ShK(L5) to healthy rats for 5 days and observed no clinical signs of toxicity, and no toxicity was seen when healthy rats received a single injection of 1000 $\mu\text{g/kg}$ ShK(L5). The situation is less sanguine when the blood-brain-barrier is compromised as happens in EAE and MS. Rats with EAE that received ShK(L5) 10 $\mu\text{g/kg/day}$ for 10 days showed no signs of toxicity. In contrast, forty percent of rats (5/12) administered 600 $\mu\text{g/kg/day}$ for five days died on the fifth day when they developed clinical signs of EAE (extrapolated $\text{LD}_{50} = 750 \mu\text{g/kg/day}$). Since the

peak concentration of ShK(L5) in the serum (12 nM) after administration of a single injection of 200 µg/kg is sufficient to block >50% of Kv1.1 channels, toxicity observed in EAE rats administered 600 µg/kg/day ShK(L5) is likely due to the ingress into the brain of sufficient amounts of ShK(L5) to block Kv1.1. Thus, the effective therapeutic safety index of ShK(L5) is well in excess of 100 in situations where the blood-brain barrier is not compromised (as seen in autoimmune diseases that do NOT affect the central nervous system (CNS)), whereas the therapeutic safety index is 75 when the blood-brain barrier is breached.

ShK(L5) prevents and treats acute adoptive EAE and prevents DTH in Lewis rats.

ShK(L5) was evaluated for immunosuppressive activity *in vivo* in two animal models. We tested its ability to prevent and treat acute EAE induced by the transfer of MBP-activated PAS T_{EM} cells into Lewis rats (Beeton et al., 2001a; Beeton et al., 2001b; Beraud et al., 1993), as well as to suppress the DTH reaction mediated by T_{EM} cells (Soler et al., 2003). PAS cells were activated with MBP for 48 hours *in vitro* and then adoptively transferred (6-8 x 10⁶ viable cells) into Lewis rats. For the prevention trial, rats then received subcutaneous injections of saline (controls) or ShK(L5) (10 µg/kg/day) for 5 days. In the first prevention trial control rats developed mild EAE (mean maximum clinical score 2.0 ± 1.2) with an average onset of 5.6 ± 0.6 days (not shown). ShK(L5) reduced disease severity (mean maximum clinical score 0.7 ± 0.6, *p* < 0.05). In the second prevention trial, control rats developed more severe EAE (mean maximum clinical score 3.2 ± 0.4) with a mean onset of 4.8 ± 0.4 days (Fig. 5A). ShK(L5) significantly reduced disease severity (mean maximum clinical score 0.6 ± 0.4, *p* < 0.007) but did not significantly delay disease onset (5.5 ± 0.7 days; *p* = 0.07). No signs of toxicity were noted in these studies.

In the treatment trial (Fig. 5B) rats were injected with MBP-activated PAS cells, administered saline or 10 $\mu\text{g/kg/day}$ ShK(L5) when they initially developed signs of EAE (limp tail, hunched posture and loss of 6% or more of their weight over 24 hours) and therapy was continued for three days. Clinical signs of EAE peaked on day 6 in the control group (score = 3.9 ± 0.7) and on day 7 in the treated group (score = 1.9 ± 0.9 ; $p < 0.05$).

As an independent assessment of ShK(L5)'s immunosuppressive activity *in vivo*, we also examined its effectiveness in inhibiting the DTH reaction that is mediated predominantly by skin-homing T_{EM} cells (Soler et al., 2003). Lewis rats immunized with ovalbumin and adjuvant were challenged 7 days later with ovalbumin in one ear and saline in the other ear. Rats then received injections of saline (controls) or ShK(L5) (10 $\mu\text{g/kg/day}$) and ear thickness was measured as an indication of DTH. All control rats developed ear swelling 24 and 48 hours after ovalbumin challenge while the DTH reaction was substantially milder in ShK(L5)-treated animals (Fig. 5C). Thus, ShK(L5) inhibits the T_{EM} -mediated DTH response, and prevents and ameliorates severe adoptive EAE induced by myelin-activated T_{EM} cells.

Discussion

We have developed a highly specific Kv1.3 inhibitor by attaching the negatively charged amino acid L-*p*Tyr to the N-terminus of ShK via a 20 Å long hydrophilic linker. ShK(L5) blocks Kv1.3 with a K_d of 69 pM and exhibits 100-fold selectivity for Kv1.3 over Kv1.1, 260-fold selectivity over Kv1.6, 280-fold selectivity over Kv3.2, 680-fold selectivity over Kv1.2 and greater than 1000-fold selectivity over all other channels tested. Other known blockers of Kv1.3 are significantly less selective than ShK(L5). Margatoxin, a peptide from *Centruroides margaritatus* scorpion venom, suppresses DTH in mini-pigs (Koo et al., 1997) but exhibits only 5-fold selectivity for Kv1.3 (K_d 110 pM) over Kv1.2 (K_d 520 pM) and 9-fold selectivity over Kv1.1 (K_d = 10 nM). Kaliotoxin from the scorpion *Androctonus mauretanicus* suppresses DTH in rats and ameliorates EAE (Beeton et al., 2001a) and inflammatory bone resorption in experimental periodontal disease (Valverde et al., 2004), but it is less potent (Kv1.3 K_d 650 pM) and less selective (Grissmer et al., 1994) than ShK(L5). The first small molecule Kv1.3 blockers with nanomolar affinity that were discovered - iminodihydroquinolines WIN-17317 and CP-339818 and the benzhydryl piperidine UK-78,282 - also block sodium channels (Wanner et al., 1999) and the neuronal Kv1.4 channel (Hanson et al., 1999). The small molecule Kv1.3 inhibitors developed by Merck - correolide (Bao et al., 2005; Felix et al., 1999; Hanner et al., 1999; Koo et al., 1999), cyclohexyl-substituted benzamides (Schmalhofer et al., 2002) and Candelalides A-C (Singh et al., 2001) - are poorly selective for Kv1.3. Psora-4, the most potent small-molecule Kv1.3 blocker (K_d = 3 nM) is only 16-20 fold selective for Kv1.3 over Kv1.1 and Kv1.2, and 2.5-fold selective over the cardiac Kv1.5 channel (Vennekamp et al., 2004). Luteolin, a flavinoid that ameliorates EAE in rats (Hendriks et al., 2004), is sold as a nutraceutical (www.lutimax.com; www.SYNORx) ostensibly because of its ability to block Kv1.3 channels

(Lahey and Rajadhyaksha, 2004). However, luteolin is a weak Kv1.3 inhibitor ($K_d = 65 \mu\text{M}$) and it is not selective for Kv1.3 over Kv1.1, Kv1.2 or Kv1.5. Other known Kv1.3 small molecule blockers - sulfamidebenzamidoindanes (Castle et al., 2000), dichlorophenylpyrazolopyrimidines (Vaccaro et al., 2001), furoquinoline Ibu-8 (Butenschon et al., 2001), tetraphenylporphyrins (Gradl et al., 2003), 3-Alkyl- and 3-aryl-7H-furo[3,2-g]chromen-7-ones (Werneken Schnieder et al., 2004), and khellinone and chalcone derivatives (Baell et al., 2004) - are neither as potent nor as selective as ShK(L5). Due to their lack of Kv1.3 selectivity these blockers could potentially be neurotoxic if they entered the CNS at concentrations sufficient to block neuronal channels. The only Kv1.3 inhibitor with potency and Kv1.3-specificity comparable to ShK(L5) is the recently described synthetic analog (OSK1-Lys¹⁶Asp²⁰) of the OSK1 toxin from scorpion *Orthochirus scrobiculosus* (Mouhat et al., 2005), but its activity as an immunomodulator remains undetermined.

The exquisite Kv1.3-specificity of ShK(L5) makes it an attractive drug prospect. ShK(L5) is remarkably stable in plasma and it reached steady-state blood levels of ~300 pM following repeated single daily subcutaneous injections of 10 $\mu\text{g/kg}$. This blood concentration of ShK(L5) is sufficient to block >90% of Kv1.3 channels without affecting other ion channels, and to cause 60-70% suppression of T_{EM} cells while sparing naïve/T_{CM} cells. A concentration of ShK(L5) greater than 1200 times its pharmacological dose was not cytotoxic or mutagenic *in vitro*. ShK(L5) did not block the cardiac Kv11.1 (HERG) K⁺ channel responsible for drug-induced Long QT syndrome (Recanatini et al., 2005), and *in vivo* administration of ShK(L5) at pharmacological concentrations (10 $\mu\text{g/kg/day}$) did not alter cardiac function in healthy rats based on continuous EKG monitoring. Repeated *in vivo* administration of 10 $\mu\text{g/kg/day}$ ShK(L5) for 2 weeks did not change clinical chemistry or hematological profiles. Healthy animals

administered a single 1000 µg/kg/day ShK(L5) injection (100 times pharmacological dose) or repeated injections of 600 µg/kg/day for five days (60 times pharmacological dose) did not exhibit any overt signs of toxicity. These results indicate that pharmacologically relevant blood levels can be attained following single daily subcutaneous injections of ShK(L5), and the effective therapeutic safety index in healthy rats exceeds 100.

ShK(L5) may have use as a therapeutic in autoimmune diseases by preferentially targeting chronically activated autoreactive T_{EM} cells that have been implicated in MS, type-1 diabetes mellitus, rheumatoid arthritis and psoriasis (Ezawa et al., 1997; Friedrich et al., 2000; Lovett-Racke et al., 1998; Markovic-Plese et al., 2001; Scholz et al., 1998; Soler et al., 2003; Viglietta et al., 2002; Wulff et al., 2003). ShK(L5) suppressed the proliferation of human and rat T_{EM} cells (IC₅₀ = ~80pM in both cases) and inhibited IL2 production at picomolar concentrations (Figs. 2 and 3). Exogenous IL2 partially overrode this block. Human naïve/T_{CM} cells were initially 60-fold less sensitive to ShK(L5) than human T_{EM} cells, and became completely resistant to the blocker during activation (Fig. 2) presumably by up-regulating K_{Ca}3.1 (Ghanshani et al., 2000; Wulff et al., 2003). Rat naïve/T_{CM} cells were 1000-fold less sensitive to ShK(L5) than T_{EM} cells. This species variation in ShK(L5)-sensitivity of naïve/T_{CM} cells compared with T_{EM} cells – 60-fold lower in humans and 1000-fold lower in rats - can be explained by differences in K⁺ channel expression between human and rat naïve/T_{CM} cells. Quiescent human naïve/T_{CM} cells express more Kv1.3 channels per cell (250-400) than K_{Ca}3.1 channels (10-20) and are therefore more potently inhibited by Kv1.3 blockers than K_{Ca}3.1 blockers (Ghanshani et al., 2000; Wulff et al., 2003). Quiescent rat naïve/T_{CM} cells in contrast express more K_{Ca}3.1 channels per cell (10-20) than Kv1.3 channels (1-10) and are more sensitive to K_{Ca}3.1 than Kv1.3 blockers (Beeton et al., 2001b). The rat/human difference in channel expression may underlie the differential sensitivity

of rat naïve/ T_{CM} cells ($IC_{50} = 100$ nM) and human naïve/ T_{CM} cells ($IC_{50} = 5$ nM) to ShK(L5). In summary, ShK(L5) preferentially suppresses T_{EM} cells while naïve/ T_{CM} cells are less sensitive to the blocker to begin with and then rapidly escape suppression by up-regulating KCa3.1 channels (Beeton et al., 2001b; Ghanshani et al., 2000; Wulff et al., 2003).

Human class-switched memory B cells (e.g. $CD27^+IgG^+IgD^-$) are implicated in the pathogenicity of autoimmune diseases (Corcione et al., 2004; Iglesias et al., 2001; O'Connor et al., 2001). Kv1.3 blockers preferentially suppress the proliferation of late memory B cells whereas naïve and early memory B cells ($CD27^+IgD^+$) are significantly less sensitive (Wulff et al., 2004). ShK(L5) could therefore shut down the function of T_{EM} and class-switched memory B cells that contribute to the development of autoimmune disorders. Of concern is the important role of class switched memory B cells in humoral immunity (production of IgG antibodies) and the diminished capacity to mount viable immune responses to bacterial challenges that might ensue as a result of channel-based suppression of these cells. Fortunately, human class-switched memory B cells are less sensitive to block by ShK ($IC_{50} = 1-4$ nM) than human T_{EM} cells ($IC_{50} = 80-400$ pM) because they express higher numbers of Kv1.3 channels at rest (~ 2000 /cell) than T_{EM} cells (250-400/cell) (Wulff et al., 2004). It might therefore be possible to titrate the dose of Kv1.3 blockers to preferentially suppress one or both groups of memory cells during therapy of autoimmune disease.

We evaluated ShK(L5) in two rat models of T_{EM} cell-induced disease, EAE induced by adoptive transfer of myelin-specific T_{EM} cells (Beeton et al., 2001b) and DTH caused by skin-homing T cells (Soler et al., 2003). ShK(L5) prevented EAE if administered as single daily injections (10 μ g/kg/day) from the time of adoptive cell transfer, and significantly reduced disease severity when therapy was initiated at the onset of symptoms. No toxicity was observed

in treated EAE rats suggesting that the blood and tissue concentrations of ShK(L5) achieved with this treatment regimen are not sufficient to block neuronal channels including heteromultimeric K_V channels containing Kv1.3 subunits (Koch et al., 1997). ShK(L5) was also effective in suppressing DTH. These proof-of-concept studies demonstrate ShK(L5)'s therapeutic effectiveness in ameliorating T_{EM}-mediated diseases in rat models. We determined ShK(L5)'s therapeutic safety index in EAE rats (when the blood-brain-barrier is likely to be compromised) by administering daily injections of a dose (600 µg/kg/day) 60-fold higher than the therapeutically effective dose. Forty percent of rats with EAE that received this dose died on the fifth day (extrapolated LD₅₀ = 750 µg/kg/day for five days), which corresponds to a therapeutic safety index of about 75.

In conclusion, ShK(L5) is a more selective Kv1.3 blocker than any other known inhibitor, and it might prove beneficial in autoimmune diseases by targeting both T_{EM} cells and class-switched memory B cells. Its picomolar affinity for Kv1.3 and remarkable plasma stability coupled with its high therapeutic safety index in healthy rats (>100) as well as in EAE rats (~75) bodes well for its potential use as a therapeutic immunomodulator. Single daily subcutaneous injections of ShK(L5) are effective in ameliorating EAE and preventing DTH indicating that this route of peptide delivery would be feasible for therapy.

Acknowledgments

We wish to thank Paul Munch, Suresh Raman and Daniel Homerick for excellent technical assistance.

References

- Baell JB, Gable RW, Harvey AJ, Toovey N, Herzog T, Hansel W and Wulff H (2004) Khellinone derivatives as blockers of the voltage-gated potassium channel Kv1.3: synthesis and immunosuppressive activity. *J. Med. Chem.* **47**:2326-2336.
- Bao J, Miao S, Kayser F, Kotliar AJ, Baker RK, Doss GA, Felix JP, Bugianesi RM, Slaughter RS and Kaczorowski GJ (2005) Potent Kv1.3 inhibitors from correolide--modification of the C18 position. *Bioorganic & Medicinal Chemistry Letters* **15**:447-451.
- Bardien-Kruger S, Wulff H, Arieff Z, Brink P, Chandy KG and Corfield V (2002) Characterisation of the human voltage-gated potassium channel gene, KCNA7, a candidate gene for inherited cardiac disorders, and its exclusion as cause of progressive familial heart block I (PFHBI). *Eur. J. Hum. Genet.* **10**:36-43.
- Beeton C, Barbaria J, Giraud P, Devaux J, Benoliel A, Gola M, Sabatier J, Bernard D, Crest M and Beraud E (2001a) Selective Blocking of Voltage-Gated K⁺ Channels Improves Experimental Autoimmune Encephalomyelitis and Inhibits T Cell Activation. *J. Immunol.* **166**:936-944.
- Beeton C, Wulff H, Barbaria J, Clot-Faybesse O, Pennington M, Bernard D, Cahalan M, Chandy K and Beraud E (2001b) Selective Blockade of T lymphocyte K⁺ channels ameliorates experimental autoimmune encephalomyelitis, a model for multiple sclerosis. *Proc. Natl. Acad. Sci. USA* **98**:13942-13947.
- Beeton C, Wulff H, Singh S, Botsko S, Crossley G, Gutman GA, Cahalan MD, Pennington MW and Chandy KG (2003) A novel fluorescent toxin to detect and investigate Kv1.3 channel up-regulation in chronically activated T lymphocytes. *J. Biol. Chem.* **278**:9928-9937.

- Beraud E, Balzano C, Zamora AJ, Varriale S, Bernard D and Ben-Nun A (1993) Pathogenic and non-pathogenic T lymphocytes specific for the encephalitogenic epitope of myelin basic protein: functional characteristics and vaccination properties. *J. Neuroimmunol.* **47**:41-53.
- Bunce C and Bell EB (1997) CD45RC Isoforms Define Two Types of CD4 Memory T Cells, One of which Depends on Persisting Antigen. *J. Exp. Med.* **185**:767-776.
- Butenschon I, Moller K and Hansel W (2001) Angular methoxy-substituted furo- and pyranoquinolinones as blockers of the voltage-gated potassium channel Kv1.3. *J. Med. Chem.* **44**:1249-1256.
- Castle NA, Hollinshead SP, Hughes PF, Mendoza GS, Wilson JW, Amato GS, Beaudoin S, Gross M and McNaughton-Smith G (2000) Potassium channel inhibitors. *U.S. Patent* 6083986.
- Chandy KG, DeCoursey TE, Cahalan MD, McLaughlin C and Gupta S (1984) Voltage-gated potassium channels are required for human T lymphocyte activation. *J. Exp. Med.* **160**:369-385.
- Chandy KG, Wulff H, Beeton C, Pennington M, Gutman GA and Cahalan MD (2004) K⁺ channels as targets for specific immunomodulation. *Trends Pharmacol. Sci.* **25**:280-289.
- Corcione A, Casazza S, Ferretti E, Giunti D, Zappia E, Pistorio A, Gambini C, Mancardi GL, Uccelli A and Pistoria V (2004) Recapitulation of B cell differentiation in the central nervous system of patients with multiple sclerosis. *Proc. Natl. Acad. Sci. U.S.A.* **101**:11064-11069.
- Deibler GE, Martenson RE and Kies MW (1972) Large scale preparation of myelin basic protein from central nervous tissue of several mammalian species. *Prep. Biochem.* **2**:139-165.

- Ezawa K, Yamamura M, Matsui H, Ota Z and Makino H (1997) Comparative analysis of CD45RA- and CD45RO-positive CD4⁺ T cells in peripheral blood, synovial fluid, and synovial tissue in patients with rheumatoid arthritis and osteoarthritis. *Acta Med. Okayama* **51**:25-31.
- Felix JP, Bugianesi RM, Schmalhofer WA, Borris R, Goetz MA, Hensens OD, Bao JM, Kayser F, Parsons WH, Rupprecht K, Garcia ML, Kaczorowski GJ and Slaughter RS (1999) Identification and biochemical characterization of a novel nortriterpene inhibitor of the human lymphocyte voltage-gated potassium channel, Kv1.3. *Biochemistry* **38**:4922-30.
- Friedrich M, Krammig S, Henze M, Docke WD, Sterry W and Asadullah K (2000) Flow cytometric characterization of lesional T cells in psoriasis: intracellular cytokine and surface antigen expression indicates an activated, memory/effector type 1 immunophenotype. *Arch. Dermatol. Res.* **292**:519-521.
- Fujiwara Y, Akaji K and Kiso Y (1994) Racemization-free synthesis of C-terminal cysteine-peptide using 2-chlorotrityl resin. *Chem. Pharm. Bull. (Tokyo)* **42**:724-726.
- Ghanshani S, Wulff H, Miller MJ, Rohm H, Neben A, Gutman GA, Cahalan MD and Chandy KG (2000) Up-regulation of the IKCa1 potassium channel during T-cell activation: Molecular Mechanism and functional consequences. *J. Biol. Chem.* **275**:37137-49.
- Gradl SN, Felix JP, Isacoff EY, Garcia ML and Trauner D (2003) Protein surface recognition by rational design: nanomolar ligands for potassium channels. *J. Am. Chem. Soc.* **125**:12668-12669.
- Grissmer S, Nguyen AN, Aiyar J, Hanson DC, Mather RJ, Gutman GA, Karmilowicz MJ, Auperin DD and Chandy KG (1994) Pharmacological characterization of five cloned

voltage-gated K⁺ channels, types Kv1.1, 1.2, 1.3, 1.5, and 3.1, stably expressed in mammalian cell lines. *Mol. Pharmacol.* **45**:1227-1234.

Gutman GA, Chandy KG, Adelman JP, Aiyar J, Bayliss DA, Clapham DE, Covarrubias M, Desir GV, Furuichi K, Ganetzky B, Garcia ML, Grissmer S, Jan LY, Karschin A, Kim D, Kuperschmidt S, Kurachi Y, Lazdunski M, Lesage F, Lester HA, McKinnon D, Nichols CG, O'Kelly I, Robbins J, Robertson GA, Rudy B, Sanguinetti M, Seino S, Stuehmer W, Tamkun MM, Vandenberg CA, Wei A, Wulff H and Wymore RS (2003) International Union of Pharmacology. XLI. Compendium of Voltage-Gated Ion Channels: Potassium Channels. *Pharmacol. Rev.* **55**:583-586.

Hammerschmidt F and Hanbauer M (2000) Transformation of arylmethyamines into alpha-aminophosphonic acids via metalated phosphoramidates: rearrangements of partly configurationally stable N-phosphorylated alpha-aminocarbanions. *J. Org. Chem.* **65**:6121-6131.

Hanner M, Schmalhofer WA, Green B, Bordallo C, Liu J, Slaughter RS, Kaczorowski GJ and Garcia ML (1999) Binding of correolide to Kv1 family potassium channels. *J. Biol. Chem.* **274**:25237-25244.

Hanson DC, Nguyen A, Mather RJ, Rauer H, Koch K, Burgess LE, Rizzi JP, Donovan CB, Bruns MJ, Canniff PC, Cunningham AC, Verdries KA, Mena E, Kath JC, Gutman GA, Cahalan MD, Grissmer S and Chandy KG (1999) UK-78,282, a novel piperidine compound that potently blocks the Kv1.3 voltage-gated potassium channel and inhibits human T cell activation. *Br J Pharmacol* **126**:1707-1716.

- Hendriks JJA, Alblas J, van der Pol SMA, van Tol EAF, Dijkstra CD and de Vries HE (2004) Flavonoids Influence Monocytic GTPase Activity and Are Protective in Experimental Allergic Encephalitis. *J. Exp. Med.* **200**:1667-1672.
- Iglesias A, Bauer J, Litzenburger T, Schubart A and Linington C (2001) T- and B-cell responses to myelin oligodendrocyte glycoprotein in experimental autoimmune encephalomyelitis and multiple sclerosis. *Glia* **36**:220-234.
- Kalman K, Pennington MW, Lanigan MD, Nguyen A, Rauer H, Mahnir V, Paschetto K, Kem WR, Grissmer S, Gutman GA, Christian EP, Cahalan MD, Norton RS and Chandy KG (1998) ShK-Dap²², a potent Kv1.3-specific immunosuppressive polypeptide. *J. Biol. Chem.* **273**:32697-32707.
- King DS, Fields CG and Fields GB (1990) A cleavage method which minimizes side reactions following Fmoc solid phase peptide synthesis. *Int. J. Pept. Protein Res.* **36**:255-266.
- Koch RO, Wanner SG, Koschak A, Hanner M, Schwarzer C, Kaczorowski GJ, Slaughter RS, Garcia ML and Knaus HG (1997) Complex subunit assembly of neuronal voltage-gated K⁺ channels. Basis for high-affinity toxin interactions and pharmacology. *J. Biol. Chem.* **272**:27577-27581.
- Kolski-Andreaco A, Tomita H, Shakkottai VG, Gutman GA, Cahalan MD, Gargus JJ and Chandy KG (2004) SK3-1C, a dominant-negative suppressor of SK_{Ca} and IK_{Ca} channels. *J. Biol. Chem.* **279**:6893-6904.
- Koo GC, Blake JT, Shah K, Staruch MJ, Dumont F, Wunderler D, Sanchez M, McManus OB, Sirotina-Meisher A, Fischer P, Boltz RC, Goetz MA, Baker R, Bao J, Kayser F, Rupprecht KM, Parsons WH, Tong XC, Ita IE, Pivnichny J, Vincent S, Cunningham P, Hora DJ, Feeney W, Kaczorowski G and et al. (1999) Correolide and derivatives are

- novel immunosuppressants blocking the lymphocyte Kv1.3 potassium channels. *Cell. Immunol.* **197**:99-107.
- Koo GC, Blake JT, Talento A, Nguyen M, Lin S, Sirotina A, Shah K, Mulvany K, Hora D, Jr., Cunningham P, Wunderler DL, McManus OB, Slaughter R, Bugianesi R, Felix J, Garcia M, Williamson J, Kaczorowski G, Sigal NH, Springer MS and Feeney W (1997) Blockade of the voltage-gated potassium channel Kv1.3 inhibits immune responses in vivo. *J. Immunol.* **158**:5120-5128.
- Lahey T and Rajadhyaksha VJ (2004) 3-Deoxyflavonoid inhibition of T-lymphocyte activation, and therapeutic use, pp 19, US patent 2004102386.
- Lin CS, Boltz RC, Blake JT, Nguyen M, Talento A, Fischer PA, Springer MS, Sigal NH, Slaughter RS, Garcia ML, Kaczorowski G and Koo G (1993) Voltage-gated potassium channels regulate calcium-dependent pathways involved in human T lymphocyte activation. *J. Exp. Med.* **177**:637-645.
- Lovett-Racke AE, Trotter JL, Lauber J, Perrin PJ, June CH and Racke MK (1998) Decreased dependence of myelin basic protein-reactive T cells on CD28-mediated costimulation in multiple sclerosis patients: a marker of activated/memory T cells. *J. Clin. Invest.* **101**:725-730.
- Markovic-Plese S, Cortese I, Wandinger KP, McFarland HF and Martin R (2001) CD4⁺CD28⁻ costimulation-independent T cells in multiple sclerosis. *J. Clin. Invest.* **108**:1185-1194.
- Middleton RE, Sanchez M, Linde AR, Bugianesi RM, Dai G, Felix JP, Koprak SL, Staruch MJ, Bruguera M, Cox R, Ghosh A, Hwang J, Jones S, Kohler M, Slaughter RS, McManus OB, Kaczorowski GJ, Garcia ML. (2003). Substitution of a single residue in

- Stichodactyla helianthus peptide, ShK-Dap²², reveals a novel pharmacological profile. *Biochemistry*. **42**:13698-13707.
- Mouhat S, Visan V, Ananthakrishnan S, Wulff H, Andreotti N, Grissmer S, Darbon H, De Waard M, Sabatier JM (2005). K⁺ channel types targeted by synthetic OSK1, a toxin from *Orthochirus scrobiculosus* scorpion venom. *Biochem J*. **385**:95-104
- Nicolas E, Vilaseca M and Giralt E (1995) A study of the use of NH₄I for the reduction of methionine sulfoxide in peptides containing cysteine and cystine. *Tetrahedron* **51**:5701-5710.
- O'Connor K, Bar-Or A and Hafler DA (2001) The neuroimmunology of multiple sclerosis: possible roles of T and B lymphocytes in immunopathogenesis. *J. Clin. Immunol.* **21**:81-92.
- Pennington M, Byrnes M, Zaydenberg I, Khaytin I, de Chastonay J, Krafte D, Hill R, Mahnir V, Volberg W, Gorczyca W and Kem W (1995) Chemical synthesis and characterization of ShK toxin: a potent potassium channel inhibitor from a sea anemone. *Int. J. Pept. Protein Res.* **346**:354-358.
- Pennington M, Mahnir V, Khaytin I, Zaydenberg I, Byrnes M and Kem W (1996a) An essential binding surface for ShK toxin interaction with rat brain potassium channels. *Biochemistry* **35**:16407-16411.
- Pennington M, Mahnir V, Krafte D, Zaydenberg I, Byrnes M, Khaytin I, Crowley K and Kem W (1996b) Identification of three separate binding sites on SHK toxin, a potent inhibitor of voltage-dependent potassium channels in human T-lymphocytes and rat brain. *Biochem. Biophys. Res. Commun.* **219**:696-701.

- Peter MJ, Varga Z, Hajdu P, Gaspar RJ, Damjanovich S, Horjales E, Possani LD and Panyi G (2001) Effects of Toxins Pi2 and Pi3 on Human T Lymphocyte Kv1.3 Channels: The Role of Glu7 and Lys24. *J. Membr. Biol.* **179**:13-25.
- Recanatini M, Poluzzi E, Masetti M, Cavalli A and De Ponti F (2005) QT prolongation through hERG K⁺ channel blockade: Current knowledge and strategies for the early prediction during drug development. *Med. Res. Rev.* **25**:133-166.
- Sallusto F, Lenig D, Forster R, Lipp M and Lanzavecchia A (1999) Two subsets of memory T lymphocytes with distinct homing potentials and effector functions. *Nature* **401**:708-712.
- Schmalhofer WA, Bao J, McManus OB, Green B, Matyskiela M, Wunderler D, Bugianesi RM, Felix JP, Hanner M, Linde-Arias AR, Ponte CG, Velasco L, Koo G, Staruch MJ, Miao S, Parsons WH, Rupprecht K, Slaughter RS, Kaczorowski GJ and Garcia ML (2002) Identification of a new class of inhibitors of the voltage-gated potassium channel, Kv1.3, with immunosuppressant properties. *Biochemistry* **41**:7781-7794.
- Scholz C, Patton KT, Anderson DE, Freeman GJ, Hafler DA. (1998) Expansion of autoreactive T cells in multiple sclerosis is independent of exogenous B7 costimulation. *J Immunol.* **160**:1532-1538
- Singh S, Zink DL, Dombrowski AW, Dezeny G, Bills GF, Felix J, Slaughter RS and Goetz MA (2001) Candelalides A-C: novel diterpenoid pyrones from fermentations of *Sesquicillium candelabrum* as blockers of the voltage-gated potassium channel Kv1.3. *Org. Lett.* **3**:247-250.
- Soler D, Humphreys TL, Spinola SM and Campbell JJ (2003) CCR4 versus CCR10 in human cutaneous TH lymphocyte trafficking. *Blood* **101**:1677-1682.

- Task Force of the European Society of Cardiology the North American Society of Pacing
Electrophysiology (1996) Heart Rate Variability: Standards of Measurement,
Physiological Interpretation, and Clinical Use. *Circulation* **93**: 1043-1065
- Tian Z, Gu C, Roeske RW, Zhou M and Van Etten RL (1993) Synthesis of phosphotyrosine-
containing peptides by solid-phase method. *Int. J. Peptide Protein Res.* **42**:155-158.
- Vaccaro W, L. Y, Atwal K, Bhandaru RS, Finley H and Lloyd J (2001) Heterocyclic
dihydropyrimidines as potassium channel inhibitors, US patent WO0140231.
- Valverde P, Kawai T and Taubman M (2004) Selective blockade of voltage-gated potassium
channels reduces inflammatory bone resorption in experimental periodontal disease. *J.*
Bone Miner. Res. **19**:155-164.
- Vennekamp J, Wulff H, Beeton C, Calabresi PA, Grissmer S, Hansel W and Chandy KG (2004)
Kv1.3 blocking 5-phenylalkoxypsoralens: a new class of immunomodulators. *Mol.*
Pharmacol. **65**:1364-1374.
- Viglietta V, Kent SC, Orban T and Hafler DA (2002) GAD65-reactive T cells are activated in
patients with autoimmune type 1a diabetes. *J. Clin. Invest.* **109**:895-903.
- Wanner SG, Glossmann H, Knaus HG, Baker R, Parsons W, Rupprecht KM, Brochu R, Cohen
CJ, Schmalhofer W, Smith M, Warren V, Garcia ML and Kaczorowski G (1999) WIN
17317-3, a new high-affinity probe for voltage-gated sodium channels. *Biochemistry*
38:11137-11146.
- Wernekschnieder A, Korner P and Hansel W (2004) 3-Alkyl- and 3-aryl-7H-furo[3,2-
g]chromen-7-ones as blockers of the voltage-gated potassium channel Kv1.3. *Pharmazie*
59:319-320.

- Wulff H, Calabresi P, Allie R, Yun S, Pennington MW, Beeton C and Chandy KG (2003) The voltage-gated Kv1.3 K⁺ channel in effector memory T cells as new target for MS. *J. Clin. Invest.* **111**:1703-1713.
- Wulff H, Knaus H, Pennington M and Chandy KG (2004) K⁺ channel expression during B cell differentiation: implications for immunomodulation and autoimmunity. *J. Immunol.* **173**:776-786.
- Wulff H, Miller MJ, Haensel W, Grissmer S, Cahalan MD and Chandy KG (2000) Design of a potent and selective inhibitor of the intermediate-conductance Ca²⁺-activated K⁺ channel, IKCa1: A potential immunosuppressant. *Proc. Natl. Acad. Sci. U.S.A.* **97**:8151-8156.
- Zhou W, Cayabyab FS, Pennefather PS, Schlichter LC and DeCoursey TE (1998) HERG-like K⁺ channels in microglia. *J. Gen. Physiol.* **111**:781-794.

Footnotes

This work was supported by grants from the National Multiple Sclerosis Society (HW, KGC, PAC, MWP), NIH (NS048252; KGC), the Arthritis National Research Foundation (CB) and a Postdoctoral Fellowship from NMSS (CB).

Reprint requests to: K. George Chandy, M.D., Ph.D., Department of Physiology and Biophysics, Medical School, 291 Irvine Hall, University of California, Irvine, Irvine, CA 92697-4561. Tel: 949-824-7435, Fax: 949-824-3143, email: gchandy@uci.edu

Legends for figures

Fig. 1. Generation of a selective Kv1.3 blocker. **A**, Molecular model of ShK based on the published NMR structure. The Lys²², critical for channel blockade, is highlighted in orange. L-*p*Tyr was attached to the α -amino group of Arg¹ of ShK (highlighted in cyan) through an Aeea linker (right). The structures of the linker and L-*p*Tyr were modeled with AM1 in Hyperchem. **B**, Effect of ShK (top) and ShK(L5) (bottom) on Kv1.3 and Kv1.1 currents in stably transfected cells. **C**, Dose-dependent inhibition of Kv1.3 (open symbols) and Kv1.1 (closed symbols) by ShK (blue) and ShK(L5) (red). K_d s on Kv1.3 = 10 ± 1 pM (ShK) and 69 ± 5 pM (ShK(L5)); K_d s on Kv1.1 = 28 ± 6 pM (ShK) and 7.4 ± 0.8 nM (ShK(L5)). **D**, Time course of wash-in and wash-out of ShK(L5) on Kv1.3. Cells were held at a holding potential of -80 mV and depolarized for 200 msec to 40 mV every 30 secs. **E**, K_d values shown for inhibition of Kv1.3 and Kv1.1 by ShK analogs. K_d s for ShK-F6CA and ShK-Dap²² are from published sources (Beeton et al., 2003; Chandy et al., 2004; Kalman et al., 1998).

Fig. 2. ShK(L5) preferentially suppresses the proliferation of human T_{EM} cells. Human PBMCs (**A**) and a human T_{EM} line (**B**) were stained with antibodies against CD3, CD45RA and CCR7. Staining intensities of CD45RA and CCR7 were determined by flow cytometry in the CD3⁺-gated population. **C**, Dose-dependent inhibition by ShK (blue) and ShK(L5) (red) of [³H] thymidine incorporation by PBMCs (open symbols, a mixture of naïve/T_{CM} cells) and T_{EM} cells (closed symbols) stimulated for 48 hours with anti-CD3 antibody. **D**, Pre-activated human PBMCs (naïve/T_{CM} cells) that up-regulate KCa3.1 expression (Ghanshani et al., 2000) become resistant to ShK(L5) inhibition when reactivated with anti-CD3 antibody. These cells have

previously been shown to become sensitive to the $K_{Ca}3.1$ -specific inhibitor TRAM-34 (Ghanshani et al., 2000).

Fig. 3. ShK(L5) preferentially suppresses the proliferation of rat T_{EM} cells. **A**, CD45RC staining of rat splenic T cells (left) and PAS T cells (right) detected by flow cytometry. **B**, Kv1.3 currents exhibited by quiescent (top) and myelin antigen-activated (bottom) PAS T cells. **C**, Flow cytometry profiles of ShK-F6CA-staining in quiescent (top) and myelin antigen-activated (bottom) PAS T cells. Unstained cells (black lines) and cells stained with ShK-F6CA (green filled). Competition of ShK-F6CA staining by unlabeled ShK(L5) is red-filled. **D**, Confocal images of Kv1.3 immunostaining in quiescent (top) and myelin antigen-activated (bottom) PAS T cells. Statistical analysis was carried out using the Mann-Whitney *U*-test. **E**, Dose-dependent inhibition by ShK (blue) and ShK(L5) (red) of [3 H] thymidine incorporation by rat (left) naïve/ T_{CM} (open symbols) and T_{EM} (closed symbols) cells activated with Con A (1 μ g/ml). **F**, Dose-dependent inhibition by ShK (blue) and ShK(L5) (red) of IL2 secretion by PAS T cells 7 hours after stimulation with MBP. **G**, ShK(L5)-induced inhibition of myelin-antigen triggered [3 H] thymidine incorporation by PAS T cells (open symbols) is reversed by the addition of 20 u/ml IL2 (closed symbols).

Fig. 4. Circulating half-life and stability of ShK(L5). **A**, Known amounts of ShK(L5) were added to rat serum (Δ) or to PBS (\blacksquare) and blocking activity was determined on Kv1.3 channels stably expressed in L929 cells. **B**, A single dose of 200 μ g/kg of ShK(L5) was injected subcutaneously into 4 rats. Blood was drawn at the indicated times and serum was tested by patch-clamp to determine the amount of ShK(L5). **C**, Data fitted to a single exponential decay. Half-life \approx 50 min. **D**, Five Lewis rats received single daily subcutaneous injections of 10

$\mu\text{g/kg/day}$ ShK(L5) for 5 days. Blood was drawn each morning (24 hours after the previous injection) and tested for blocking activity on Kv1.3 channels by patch-clamp. **E**, Rats received a single dose of 10 mg/kg ShK(L5) either subcutaneously (open bars; $n = 4$) or intravenously (closed bars; $n = 4$). Blood was drawn at the indicated times. Serum was tested by patch-clamp to determine the amount of ShK(L5) in blood. **F**, A half-blocking dose of ShK(L5) was added to rat plasma (\square) or to PBS containing 2% rat plasma (\blacksquare) and incubated at 37°C for varying duration. Aliquots were taken at the indicated times and blocking activity determined on Kv1.3 channels.

Fig. 5. ShK-L5 prevents DTH and acute adoptive EAE in Lewis rats. **A**, Prevention of EAE. PAS T cells were activated *in vitro*, washed, and injected intraperitoneally on day 0. Clinical scoring of EAE: 0 = no clinical signs, 0.5 = distal limps tail, 1 = limp tail, 2 = mild paraparesis or ataxia, 3 = moderate paraparesis, 4 = complete hind limb paralysis, 5 = 4 + incontinence, 6 = death. Rats ($n = 6/\text{group}$) were injected subcutaneous with vehicle (\square ; $n = 6$) or ShK(L5) (\blacksquare ; $n = 6$; $10\mu\text{g/kg/day}$) from day 0 to day 5. **B**. Treatment of EAE. PAS T cells were activated *in vitro*, washed, and injected intraperitoneally on day 0. Treatment with ShK(L5) at $10\mu\text{g/kg/day}$ was started when rats developed clinical signs of EAE and was continued for 3 days. **C**, DTH reaction was elicited against ovalbumin and rats ($n = 6/\text{group}$) were treated with ShK(L5) $10\mu\text{g/kg/day}$ for 2 days, after which ear swelling was measured. Statistical analysis was carried out using the Mann-Whitney *U*-test.

Table 1. Selectivity of ShK(L5)

Channels	K_d of ShK(L5) [pM]
Kv1.1	$7,000 \pm 1,000$
Kv1.2	$48,000 \pm 7,000$
Kv1.3 (cloned)	69 ± 5
Kv1.3 (native)	76 ± 8
Kv1.4	$137,000 \pm 3,000$
Kv1.5	100,000 no effect
Kv1.6	$18,000 \pm 3,000$
Kv1.7	100,000 no effect
Kv2.1	100,000 no effect
Kv3.1	100,000 no effect
Kv3.2	$20,000 \pm 2,000$
Kir2.1	100,000 no effect
Kv11.1 (HERG)	100,000 no effect
K _{Ca} 1.1	100,000 no effect
K _{Ca} 2.1	100,000 no effect
K _{Ca} 2.3	100,000 no effect
K _{Ca} 3.1	$115,000 \pm 5,000$
Nav1.2	100,000 no effect
Nav1.4	100,000 no effect
Swelling-activated T cell Cl ⁻ channel	100,000 no effect
Cav1.2	100,000 no effect

Table 2. Toxicity study of ShK(L5)

<i>In vitro</i> tests	100 nM ShK(L5)	
Cytotoxicity (% dead cells)		
Human PBMCs	7.5 ± 4.3	
PAS T cells	8.1 ± 0.8	
Jurkat cells	5.5 ± 3.3	
Burkitt lymphoma	3.1 ± 0.9	
RPMI 8226 myeloma	6.5 ± 2.1	
Ames Test	Negative	
Acute <i>in vivo</i> tests	Saline	ShK(L5) 10 µg/kg
Electrocardiogram*		
Heart rate	302 ± 13	311 ± 20
SDNN	13.3 ± 3.0	17.8 ± 4.4
CV%	6.7 ± 1.4	9.2 ± 2.2
SDANN _{5min}	5.0 ± 2.0	6.9 ± 2.3
rMSSD	6.8 ± 2.2	9.8 ± 3.5
HF (n.u.)	71 ± 21	79 ± 37
HF (%)	50 ± 8	53 ± 10
LF (n.u.)	68 ± 4	64 ± 10
LF (%)	50 ± 8	47 ± 10
LF/HF	1.1 ±0.4	1.3 ± 0.7
Sub-chronic <i>in vivo</i> tests	Saline	ShK(L5) 10 µg/kg/day for 2 weeks
Weight gain (%)	7.2 ± 1.8	6.2 ± 1.7
Complete blood count		
Hematocrit (%)	40.3 ± 1.4	39.0 ± 4.9
Hemoglobin (g/dl)	15.3 ± 0.5	15.0 ± 1.5
MCV (fl)	48.5 ± 0.2	48.3 ± 0.3
MCH (pg)	18.5 ± 0.8	18.5 ± 0.6
MCHC (g/dl)	38.0 ± 1.8	38.4 ± 1.3
Total white cells (x10 ³ mm ⁻³)	7.1 ± 2.1	7.1 ± 2.5
Total red cells (x10 ⁶ mm ⁻³)	8.3 ± 0.3	8.1 ± 1.0
Total platelets (x10 ³ mm ⁻³)	656 ± 214	606 ± 106
Blood chemistry		
Alkaline phosphatase (U/I)	170 ± 26	150 ± 18
Glucose (mg/dl)	139 ± 21	150 ± 18
Blood urea nitrogen (mg/dl)	17.1 ± 2.6	15.0 ± 1.7
Creatinine (mg/dl)	0.6 ± 0	0.6 ± 0.1
Albumin (g/dl)	5.0 ± 0.3	4.5 ± 0.4
Thymic cell populations (%)		
CD4 ⁺ CD8 ⁻	3.6 ± 1.1	4.3 ± 0.7
CD4 ⁺ CD8 ⁺	77.8 ± 6.1	76.8 ± 4.1
CD4 ⁺ CD8 ⁻	8.5 ± 1.7	11.2 ± 2.0
CD4 ⁺ CD8 ⁺	10.0 ± 3.3	7.6 ± 1.3
CD3 ⁺	89.5 ± 1.6	93.2 ± 3.5
Splenic populations (%)		
CD3 ⁺	72.4 ± 4.4	65.4 ± 0.1
CD3 ⁺ CD45RC ⁺	35.6 ± 2.6	39.8 ± 1.1
CD3 ⁺ CD45RC ⁻	23.6 ± 2.3	26.5 ± 1.3
CD3 ⁺ CD4 ⁺	62.7 ± 0.1	66.6 ± 1.2
CD3 ⁺ CD8 ⁺	26.9 ± 0.1	25.0 ± 0.2
IgM ⁺	38.8 ± 1.5	33.3 ± 0.3

Data expressed as mean ± SD. *Tested with t-tests, p<0.05 on all parameters; SDNN: Standard deviation of all normal-to-normal RR intervals; CV%: 100 x SDNN/average RR interval; SDANN_{5min}: Standard deviation of the mean of normal RR intervals for each 5 min period; rMSSD: Root mean square of successive difference; HF (n.u.): High frequency (0.75 – 2.5 Hz) power in normalized unit; LF (n.u.): Low frequency (0.2 – 0.75 Hz) power in normalized unit.

Figure 1

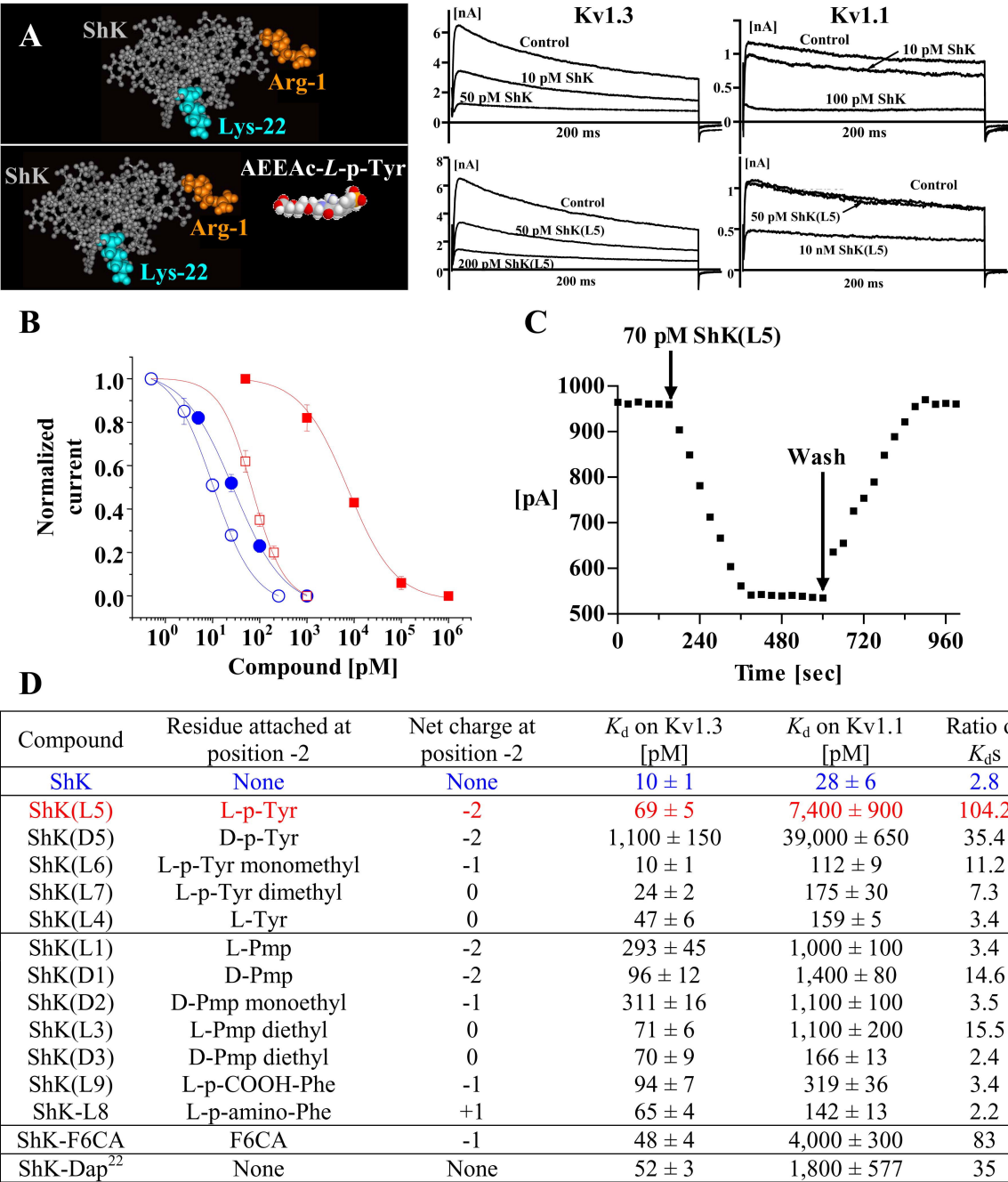


Figure 2

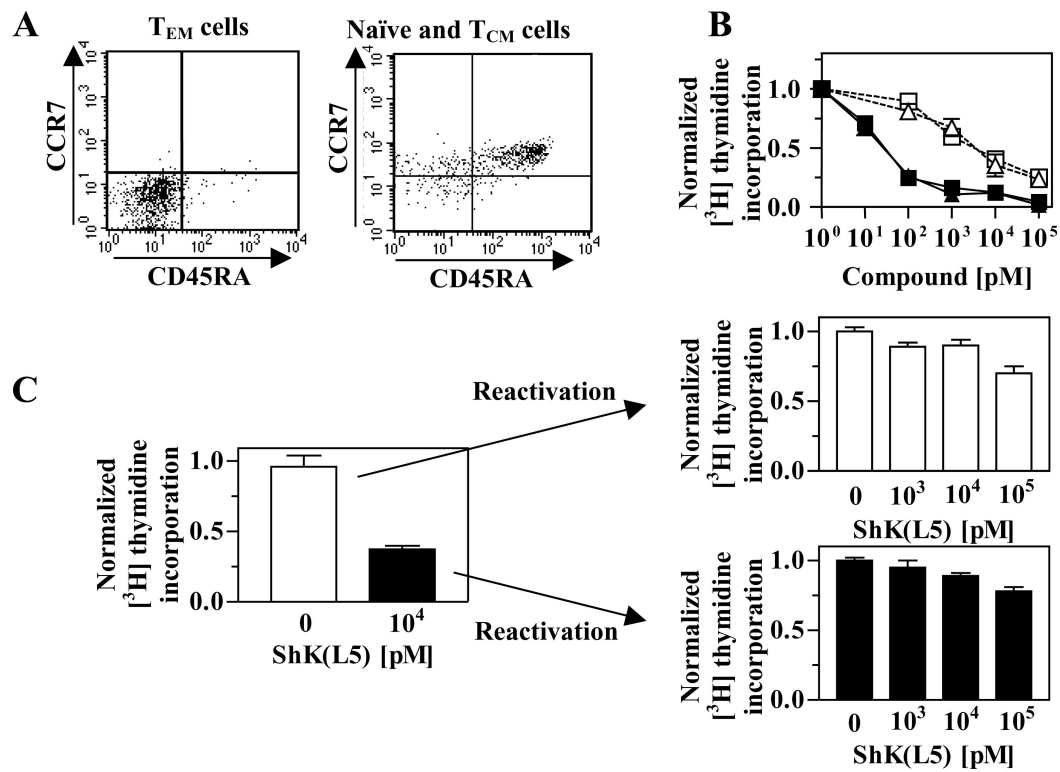
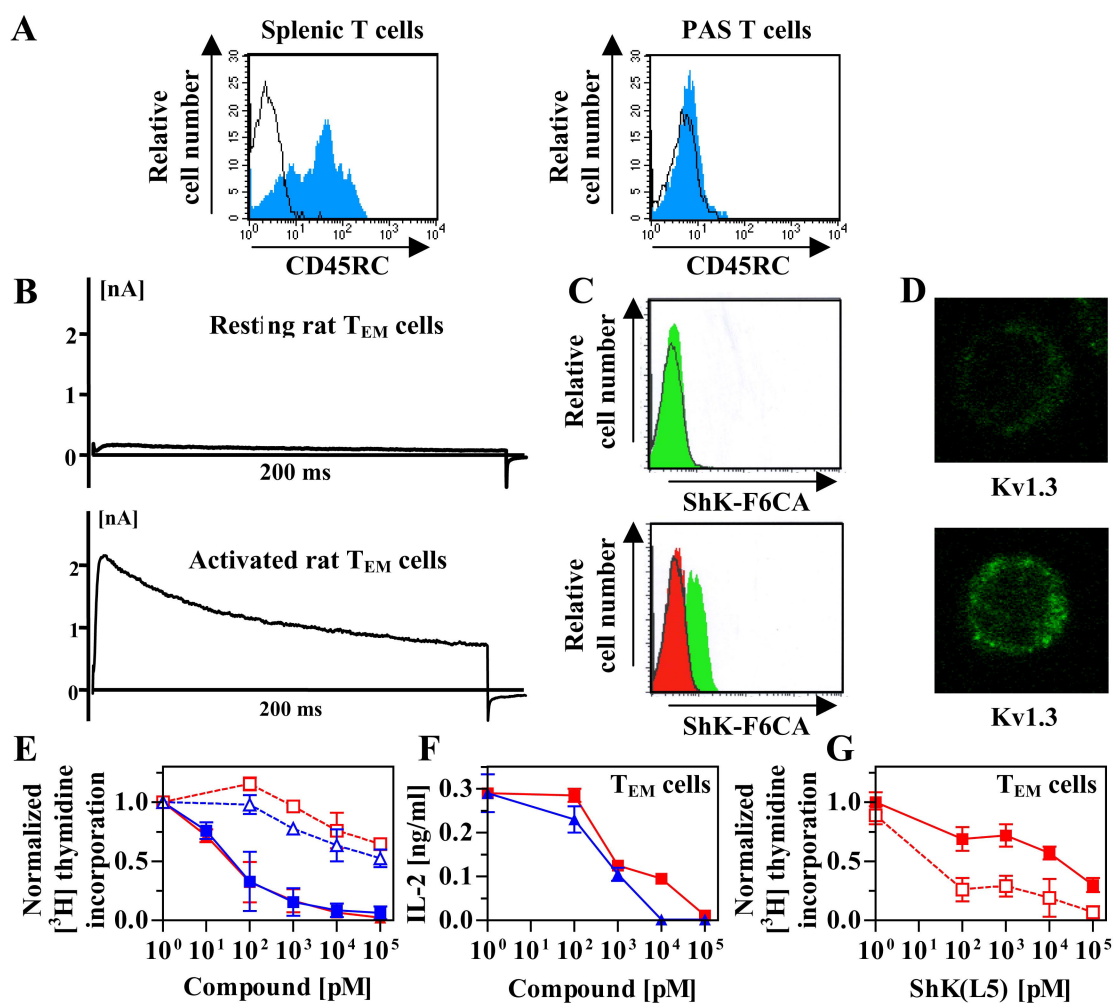


Figure 3



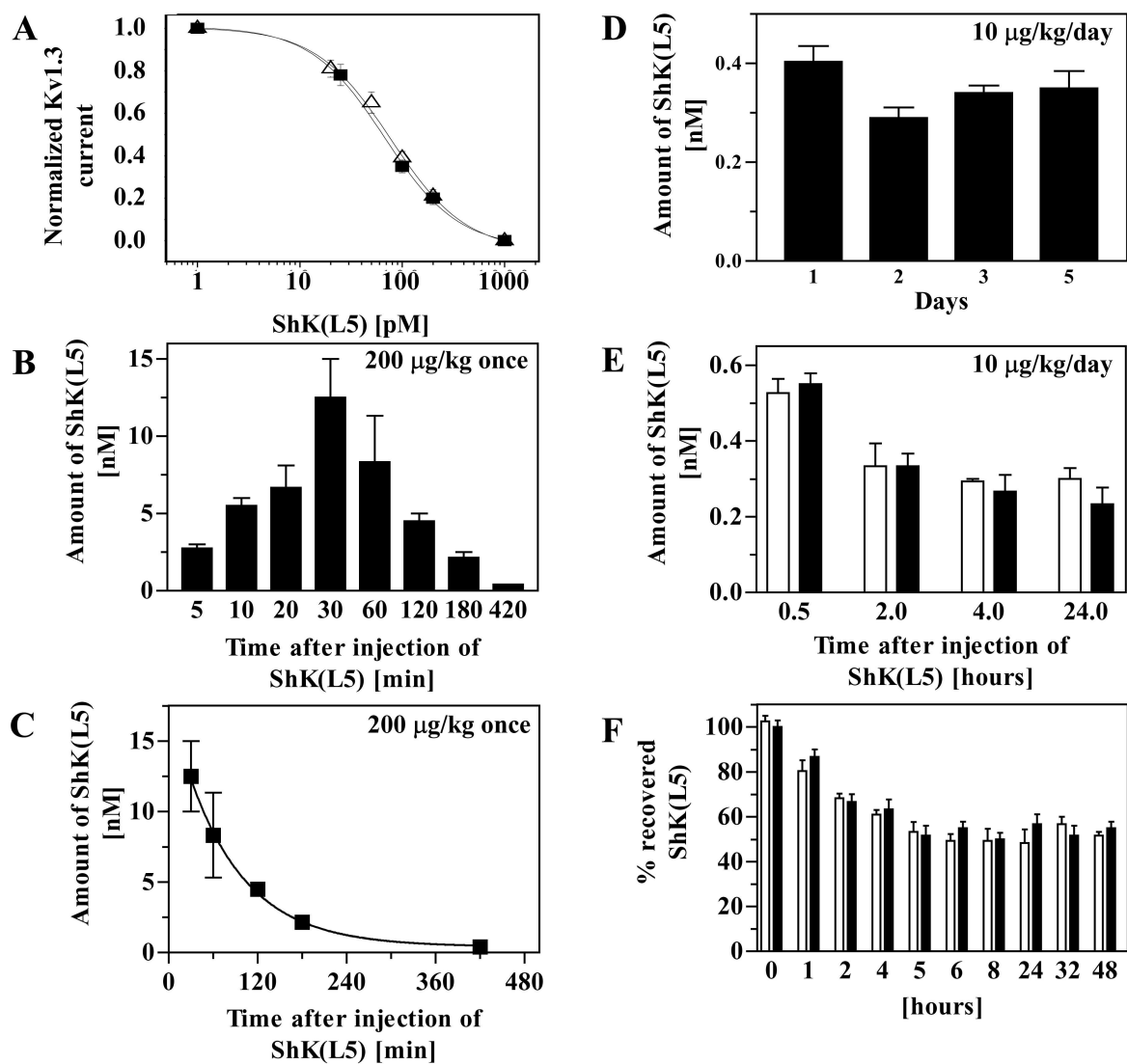


Figure 4

Figure 5

